Electrophoresis of an Ellipsoid along the Axis of a Cylindrical Pore: Effect of a Charged Boundary

Shiojenn Tseng, and Chia-Hua ChoZheng-Syun ChenJyh-Ping Hsu

Langmuir, **2008**, 24 (6), 2929-2937 • DOI: 10.1021/la703195f

Langmuir

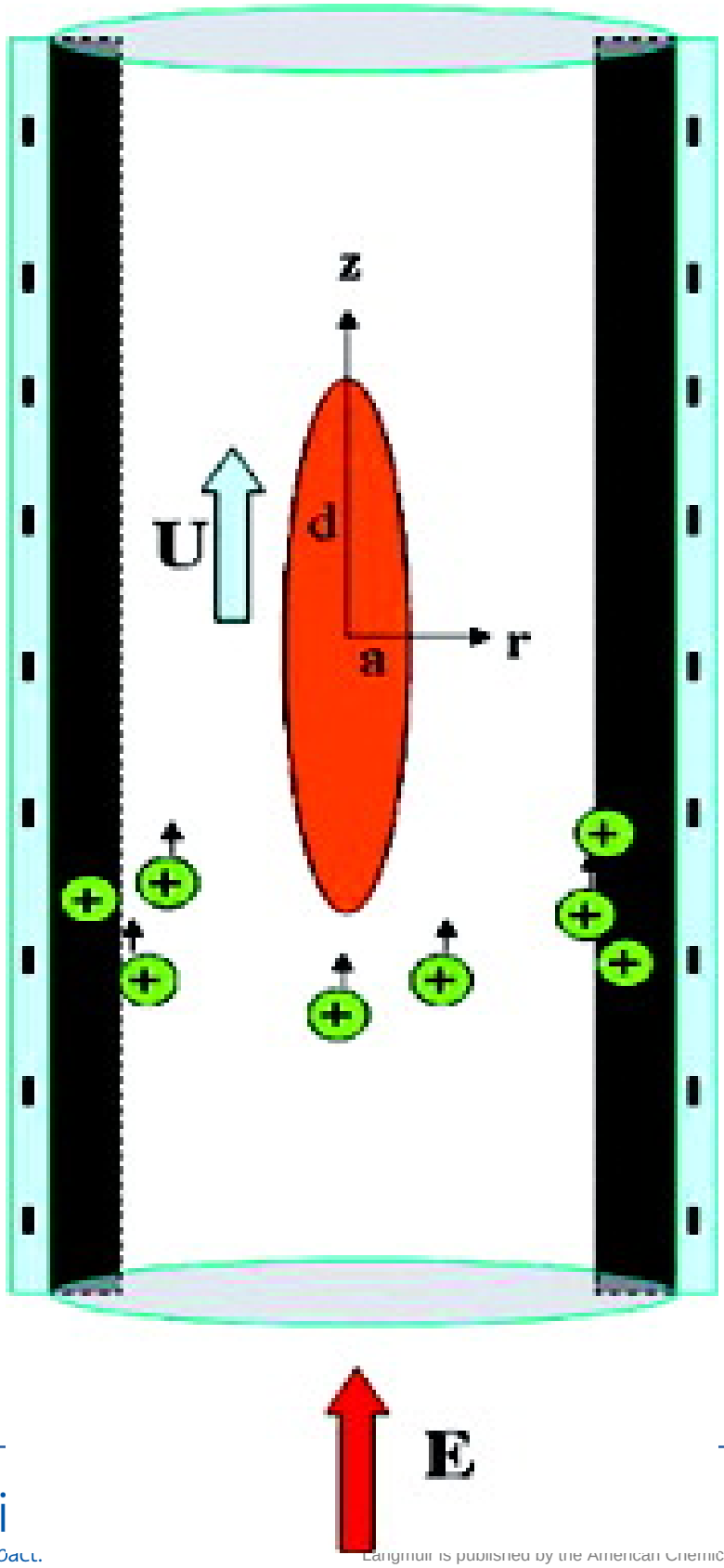

Langmuir is published by the American Chemical Society. 1155 Sixteenth Street N.W., Washington, DC 20036

Electrophoresis of an Ellipsoid along the Axis of a Cylindrical Pore: Effect of a Charged Boundary

Shiojenn Tseng and Chia-Hua Cho

Department of Mathematics, Tamkang University, Tamsui, Taipei, Taiwan 25137

Zheng-Syun Chen

Department of Chemical Engineering, National Taiwan University, Taipei, Taiwan 10617

Jyh-Ping Hsu*

Department of Chemical Engineering and Institute of Polymer Science and Engineering, National Taiwan University, Taipei, Taiwan 10617

Received October 15, 2007. In Final Form: December 2, 2007

The influence of a charged boundary on the electrophoretic behavior of a particle is investigated by considering the electrophoresis of a nonconducting ellipsoid along the axis of a cylindrical pore at the level of the linear Poisson−Boltzmann equation ignoring the polarization effect. The problem considered simulates the electrophoresis conducted in a narrow space such as capillary electrophoresis and electrophoresis through a porous medium. Here, because the effect of electroosmotic flow can be important the electrophoretic behavior is much more complicated than that for the case where a boundary is uncharged. The influences of the thickness of double layer, the aspect ratio of an ellipsoid, the relative radius of a pore, and the charge conditions on the ellipsoid and pore surfaces on the mobility of the ellipsoid are discussed. Several interesting but nonintuitive electrophoretic behaviors are observed.

Introduction

Electrophoresis, one of the electrokinetic phenomena, has been applied widely in numerous areas both as an analytical tool and as a separation technique. Modern techniques such as electrophoresis display, protein separation, and DNA analysis, to name a few, all involve this phenomenon. Relevant literature about electrokinetic phenomena dates back to as early as 1809.[1] Using a microscope, Quincke[2] was able to observe the electroosmotic flow in a glass capillary. Helmholtz[3] originated the theoretical analysis on electrophoresis and eletroosmosis by neglecting the effect of the dielectric constant of a liquid medium. This effect was considered by Smoluchowski[4] in a study of the electrophoresis of an isolated rigid sphere of constant surface potential in an infinite electrolyte solution. He derived, for the case of an infinitely thin double layer, the relation

$$\mu = \frac{v}{\mathrm{E}} = \frac{\epsilon\zeta}{\eta} \tag{1}$$

where v and E are the electrophoretic velocity of the sphere and the strength of the applied electric field, respectively, and μ, ζ, ϵ, and η are the electrophoretic mobility, the surface (zeta) potential of the sphere, and the dielectric constant and the viscosity of the electrolyte solution, respectively. If the double layer is infinitely thick, then it can be shown that[5]

$$\mu = \frac{2}{3}\frac{\epsilon\zeta}{\eta} \tag{2}$$

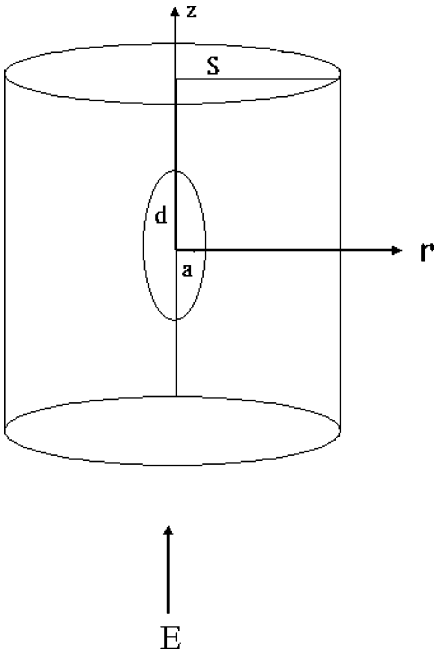

Figure 1. Electrophoresis of an ellipsoid of semi-axes d and a along the axis of a cylindrical pore of radius S, with **E** being the applied electric field. Cylindrical coordinates (r, θ, z) are adopted with the origin located at the center of the ellipsoid.

For an arbitrarily thick double layer, Henry[6] was able to derive

$$\mu = \frac{\epsilon\zeta}{\eta} f(\kappa a) \tag{3}$$

where $^1/_\kappa$ and a are the reciprocal Debye length and the radius of a particle, respectively; $f(\kappa a) = {}^2/_3$ as $\kappa a \to 0$ (infinitely thick

* Corresponding author. E-mail: jphsu@ntu.edu.tw.

(1) Reuss, F. F. *Mém. Soc. Impériale Naturalistes Moscou* **1809**, *2*, 327.
(2) Quincke, G. *Pogg. Ann.* **1861**, *113*, 513.
(3) Helmholtz, H. *Ann. Phys. Chem.* **1879**, *7*, 337.
(4) Von Smoluchowski, M. Z. *Phys. Chem.* **1918**, *92*, 129.
(5) Hückel, E. *Phys. Z.* **1924**, *25*, 204.

10.1021/la703195f CCC: $40.75
Published on Web 02/01/2008

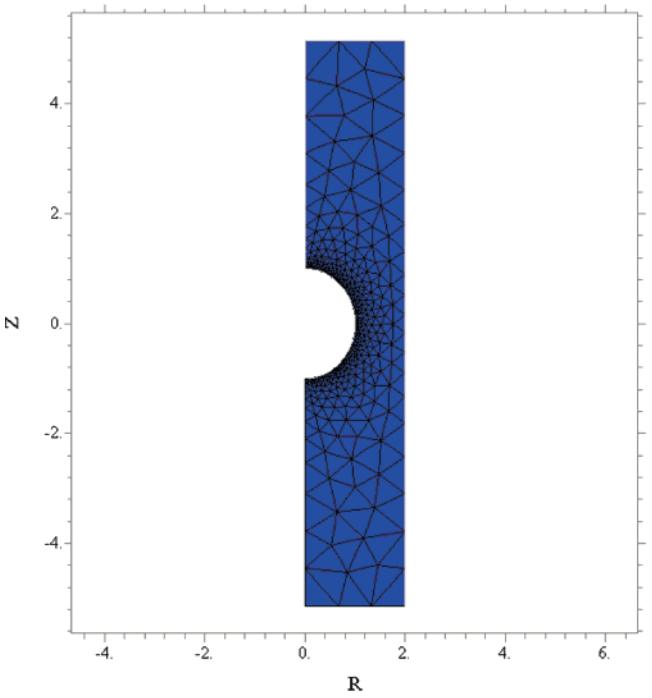

Figure 2. Typical mesh used for the case where $\zeta_p = 1$, $\zeta_w = 0$, $S = 2a_0$, and $\kappa a = 1$.

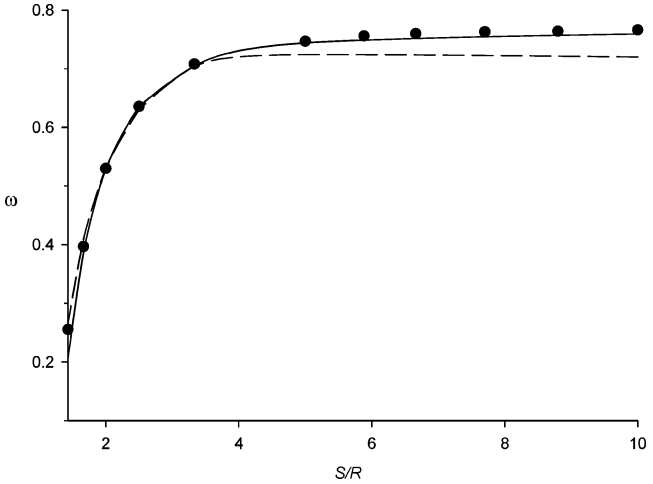

Figure 3. Variation of the scaled electrophoretic mobility ω as a function of λ for the case where a sphere of constant surface potential is placed on the axis of an uncharged cylindrical pore at $\kappa a = 4.3$. Discrete symbols, present result; dotted line, numerical result of Shugai and Carnie;[24] solid line, result of Ennis and Anderson.[23]

double layer), and $f(ka) = 1$ as $\kappa a \rightarrow \infty$ (infinitely thin double layer). Unfortunately, the double layer in practice has a finite thickness, and $f(\kappa a)$ needs to be determined through solving a set of complicated electrokinetic equations. The degree of difficulty in solving these equations depends mainly on factors such as the shape and charge conditions of a particle, the strength of the applied electric field, the thickness of double layer, and the presence of a boundary and nearby particles.

Among the shapes of a particle studied previously, the ellipsoid is relatively general because it is capable of representing a class of different particles through varying the relative lengths of its semi-major and semi-minor axes. Several attempts have been made to investigate the electrophoretic behavior of an ellipsoid. Teubner,[7] for example, analyzed the electrophoresis of an isolated ellipsoid under the condition that the effect of double-layer relaxation is negligible. General equations were derived for the force and torque acting on a rigid entity. Taking the effect of double-layer relaxation into account, O'Brien and Ward[8] studied the electrophoresis of a spheroid with a thin double layer. Yoon and Kim[9] considered the electrophoresis of an ellipsoid for the case of low surface potential, a moderately thick double layer, and a negligible effect of double-layer polarization. Their analysis was extended by Allison[10] to include the polarization effect in the electrophoretic mobility of prolate ellipsoids in an infinite medium. Keh and Huang[11] investigated the electrophoresis of colloidal spheroids under the conditions of a thin double layer with a polarization effect. Assuming a thin double layer, Feng and Wu[12] investigated the electrophoresis of an arbitrary prolate body of revolution toward an infinite conducting wall. Sun and Wu[13] considered the electrophoresis of two coaxial prolate particles for the case of a thin double layer. Hsu et al.[14] analyzed the electrophoresis of a spheroid along the axis of a cylindrical pore; the former has a low, constant surface potential, and the latter is uncharged; that is, the effect of electroosmotic flow is neglected.

The presence of a boundary has a profound influence on the electrophoretic behavior of a particle, especially if the former is charged. In particular, both the direction and the magnitude of the electrophoretic velocity of a particle can be affected appreciably by the induced electroosmotic flow near a charged surface.[15,16] The effect of a charged boundary should not be neglected in the case where electrophoresis is conducted in a narrow space, such as capillary electrophoresis and microchip electrophoresis. In the former, if a fused silica pore is used, for example, then the boundary is negatively charged because of the dissociation of the silanol group.[17−18] In the latter, if the wall surface is modified by a polymer coating, then it can be positively or negatively charged.[19] In this study, the electrophoresis of a nonconducting ellipsoid along the axis of a charged cylindrical pore is investigated. We consider the case where the surface potential is low and the effect of double-layer polarization is negligible. This extends the analysis of Hsu et al.[14] to the case where the surface of a cylindrical pore can be charged; that is, the effect of electroosmotic flow can play a role.

Theory

The problem under consideration is illustrated in Figure 1, where an ellipsoid with semi-axes d and a moves along the axis of a cylindrical pore with radius S filled with an incompressible Newtonian fluid of constant physical properties as a response to an applied electric field **E** of strength E. If $^d/_a > 1$, then the ellipsoid is an oblate; if $^d/_a = 1$, then it is a sphere;

(6) Henry, D. C. *Proc. R. Soc. London, Ser. A* **1931**, *133*, 106.
(7) Teubner, M. *J. Chem. Phys.***1982**, *76*, 5564.
(8) O'Brien, R. W.; Ward, D. N. *J. Colloid Interface Sci.* **1988**, *121*, 402.
(9) Yoon, B. J.; Kim, S. *J. Colloid Interface Sci.* **1989**, *128*, 275.
(10) Allison, S. *J. Colloid Interface Sci.* **2005**, *282*, 231.
(11) Keh, H. J.; Huang, T. Y. *J. Colloid Interface Sci.* **1993**, *160*, 354.
(12) Feng, J. J.; Wu, W. Y. *J. Fluid Mech.* **1994**, *264*, 41.
(13) Sun, K. L.; Wu, W. Y. *Int. J. Multiphase Flow* **1995**, *21*, 705.
(14) Hsu, J. P.; Huang, S. H.; Kao, C. Y.; Tseng, S. *Chem. Eng. Sci.* **2003**, *58*, 5339.
(15) Hsu, J. P.; Ku, M. H.; Kao, C. Y. *J. Colloid Interface Sci.* **2004**, *276*, 248.
(16) Zydney, A. L. *J. Colloid Interface Sci.* **1995**, *169*, 476.
(17) Bello, M. S.; de Besi, P.; Rezzonico, R.; Righetti, P. G.; Casiraghi, E. *Electrophoresis* **1994**, *15*, 623.
(18) Corradini, D. *J. Chromatogr., B* **1997**, *699*, 221.
(19) Belder, D.; Ludwig, M. *Electrophoresis* **2003**, *24*, 3595.

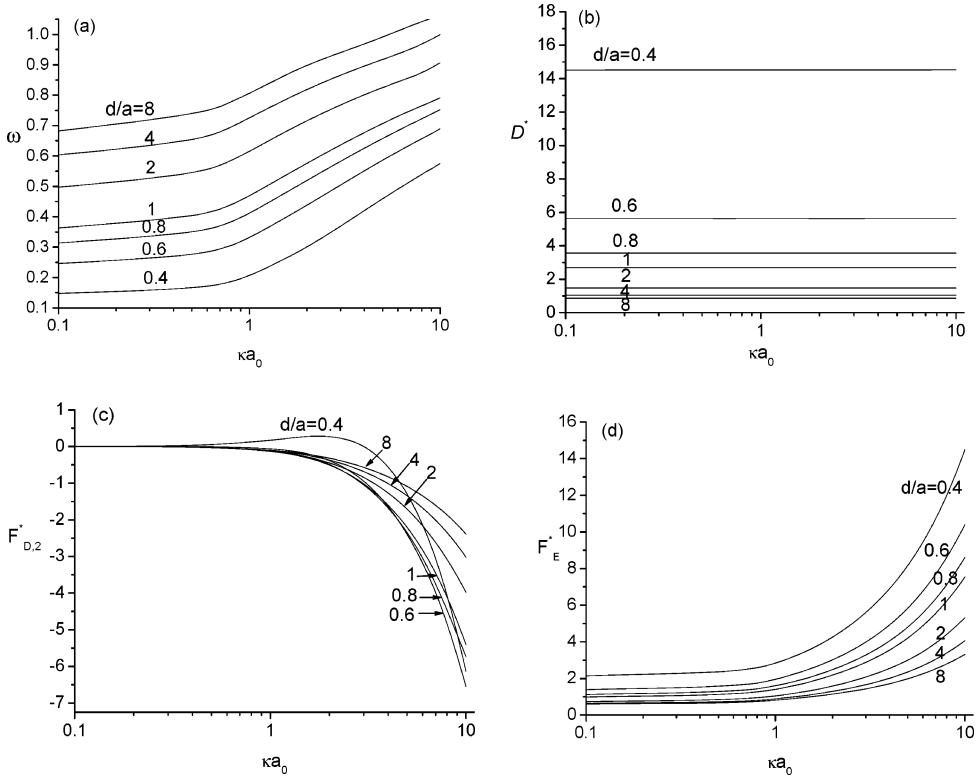

Figure 4. Variation of the scaled mobility of an ellipsoid ω (a), the scaled drag coefficient D^* (b), the scaled hydrodynamic force $F^*_{D,2}$ (c), and the scaled electric force F^*_E (d) as a function of the scaled double-layer thickness κa_0 at various values of $^d/_a$ for the case in which $\zeta_p = 1$, $\zeta_w = 0$, and $S = 3a_0$.

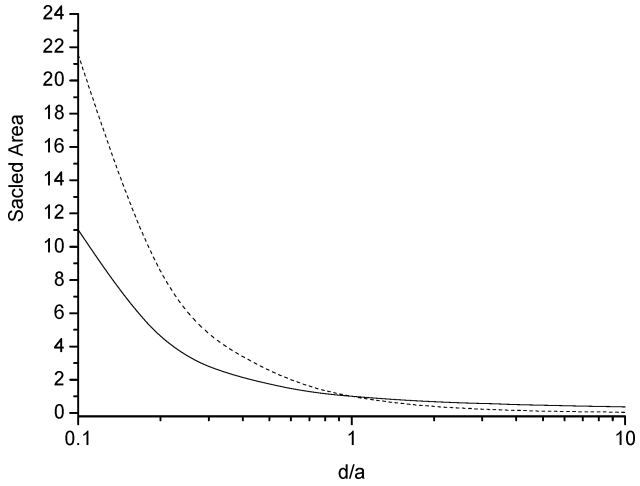

Figure 5. Variations of the scaled surface area of an ellipsoid (= surface area of an ellipsoid/surface area of the equivalent sphere, solid curve) and the scaled projection area of an ellipsoid (= projection area of an ellipsoid on the (r, θ) plane/that of the equivalent sphere $= \pi a^2/\pi a_0^2$, dashed curve) as a function of the aspect ratio $^d/_a$. The volume of an ellipsoid is fixed at $4\pi a_0^3/3$.

and if $^d/_a < 1$, then it is a prolate. Cylindrical coordinates (r, θ, z) are adopted with the origin located at the center of the ellipsoid. Because the present problem is θ-symmetric, only the (r, z) domain needs to be considered. For a simpler mathematical treatment, the electrical potential of the system under consideration Ψ is partitioned into an electrical potential in the absence of **E** or the equilibrium potential Ψ_1 and an electrical potential outside an ellipsoid arising from **E**, Ψ_2; that is, $\Psi = \Psi_1 + \Psi_2$. Suppose that Ψ is sufficiently low (lower than ca. 25 mV) and **E** is sufficiently weak (weaker than ca. 25 kV/m). Then the present problem can be described by

$$\nabla^2\Psi_1 = \kappa^2\Psi_1 \tag{4}$$

$$\nabla^2\Psi_2 = 0 \tag{5}$$

$$\eta\nabla^2\mathbf{u} - \nabla p = \rho\nabla\Psi \tag{6}$$

$$\nabla\mathbf{u} = 0 \tag{7}$$

In these expressions, ∇^2 is the Laplace operator, $\kappa = (\sum_j n_{j0}(ez_j)^2/\epsilon k_B T)^{1/2}$, n_{j0} and z_j are the bulk concentration and the valence of ionic species j, respectively, e is the elementary charge, k_B and T are the Boltzmann constant and the absolute temperature, respectively, ϵ, η, and **u** are the dielectric constant, the viscosity, and the velocity of the liquid phase, respectively, and p is the pressure.

Two types of boundary conditions are considered for the electric field. In the first case, both the surface of an ellipsoid and that of a pore are maintained at a constant surface potential. In this case, the boundary conditions associated with eqs 4 and 5 are

$$\Psi_1 = \zeta_p \text{ and } \mathbf{n}\cdot\nabla\Psi_2 = 0 \text{ on the ellipsoid surface} \tag{8}$$

$$\Psi_1 = \zeta_w \text{ and } \frac{\partial\Psi_2}{\partial r} = 0 \text{ at } r = S \tag{9}$$

$$\Psi_1 = 0 \text{ and } \nabla\Psi_2 = -\mathbf{E} \text{ as } |z| \to \infty,\ r < S \tag{10}$$

In these expressions, **n** is the unit vector pointing into the liquid phase, and ζ_p and ζ_w are the surface potential on the ellipsoid surface and that on the pore surface, respectively. Here, we assume that the equilibrium potential Ψ_1 at both ends of the pore vanish,

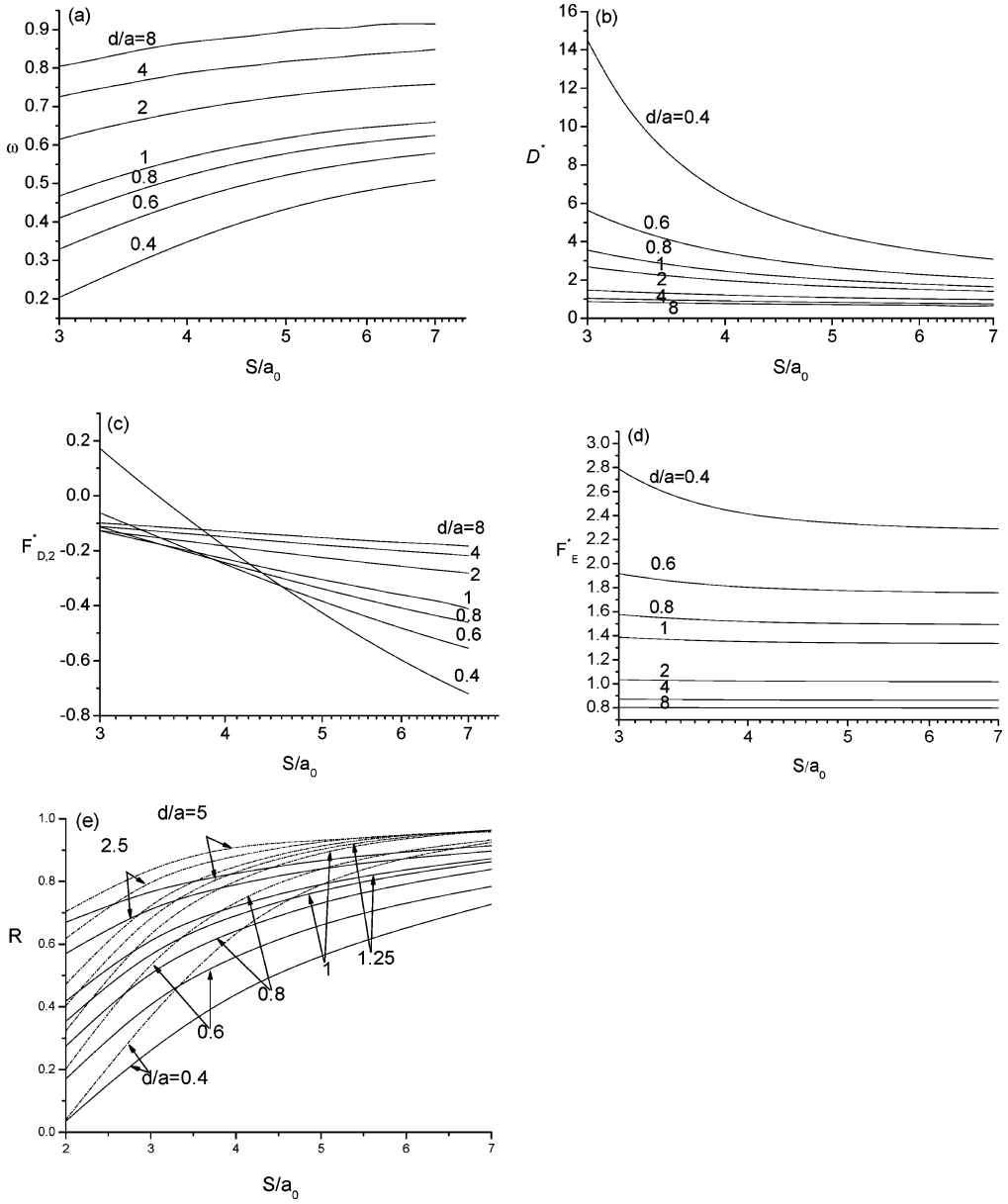

Figure 6. Variation of the scaled mobility of an ellipsoid ω (a), the scaled drag coefficient D^* (b), the scaled hydrodynamic force $F^*_{D,2}$ (c), and and the scaled electric force F^*_E (d) as a function of the scaled pore radius S/a_0 at various values of $^d/_a$ for the case in which $\zeta_p = 1$, $\zeta_w = 0$, and $\kappa a_0 = 1$. (e) Variation of the ratio $R = \omega$ (present study)/ω (Yoon and Kim)[9] as a function of S/a_0 at various combinations of $^d/_a\kappa a_0$. Dashed line, $\kappa a_0 = 1$; solid line, $\kappa a_0 = 0.2$.

both the surface of an ellipsoid surface and that of a pore are impermeable to ionic species, and the electric field at a point far away from the ellipsoid is uninfluenced by it. In the second case, we assume that the ellipsoid is maintained at a constant surface charge density σ_p and the other boundary conditions are the same as those in the first case. Therefore, the boundary conditions associated with eqs 4 and 5 include eq 10 and

$$\mathbf{n}\cdot\nabla\Psi_1 = \frac{-\sigma_p}{\epsilon} \text{ and } \mathbf{n}\cdot\nabla\Psi_2 = 0 \text{ on the ellipsoid surface} \quad (11)$$

$$\frac{\partial\Psi_1}{\partial r} = 0 \text{ and } \frac{\partial\Psi_2}{\partial r} = 0 \text{ at } r = S \quad (12)$$

Suppose that both the surface of an ellipsoid and that of the cylindrical pore are nonslip and the flow field at a point far away from the ellipsoid in the cylindrical pore is that established by electroosmotic flow. Then the boundary conditions associated with eqs 6 and 7 are

$$\mathbf{u} = U\mathbf{i}_z \text{ on the ellipsoid surface} \quad (13)$$

$$\mathbf{u} = \mathbf{0} \text{ at } r = S \text{ and as } |z| \to \infty,\ r < S \quad (14)$$

$$\mathbf{u} = u(r)\mathbf{i}_z = -\frac{\epsilon\zeta_w}{\eta}\left[1 - \frac{I_0(\kappa r)}{I_0(\kappa b)}\right]E_0\mathbf{i}z \text{ as } |z| \to \infty,\ r < b \quad (15)$$

In these expressions, U is the electrophoretic velocity of the ellipsoid, and $\mathbf{i}_z$ is the unit vector in the z direction.

In our case, the forces acting on an ellipsoid include the hydrodynamic force and the electrostatic force. To evaluate U,

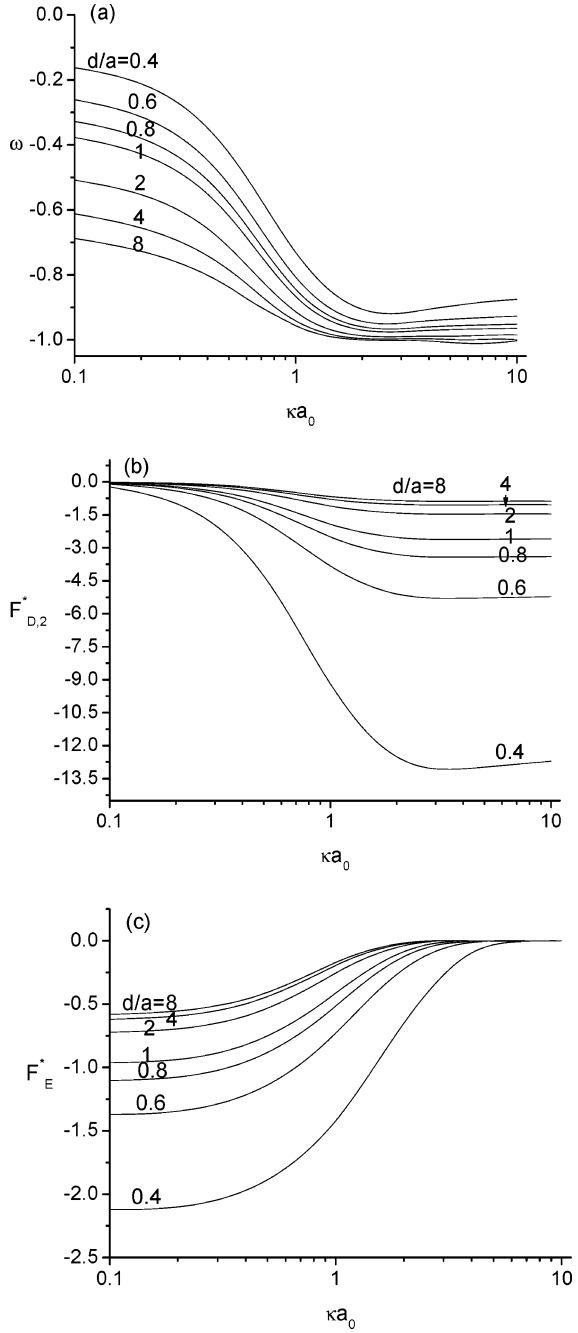

Figure 7. Variation of the scaled mobility of an ellipsoid ω (a), the scaled hydrodynamic force $F^*_{D,2}$ (b), and the scaled electric force F^*_E (c) as a function of the scaled double-layer thickness κa_0 at various values of $^d/_a$ for the case in which $\zeta_p = 0$, $\zeta_w = 1$, and $S = 3a_0$.

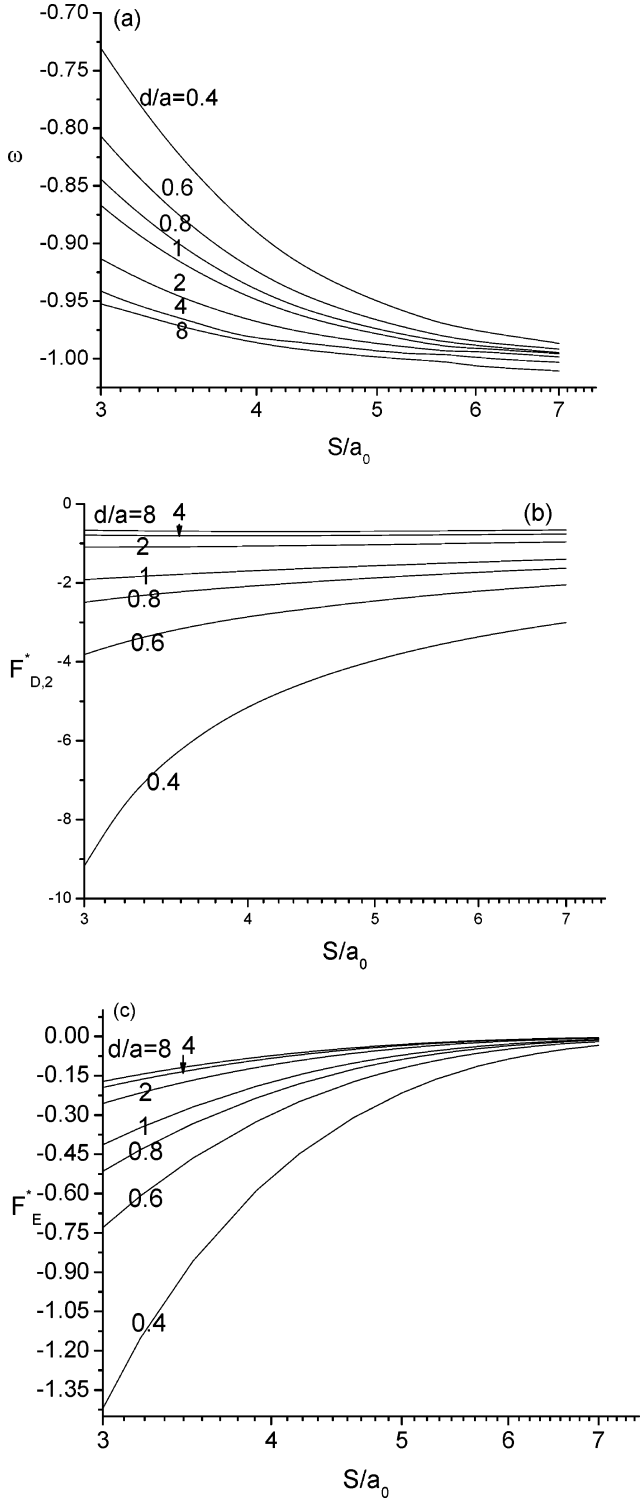

Figure 8. Variation of the scaled mobility of an ellipsoid ω (a), the scaled hydrodynamic force $F^*_{D,2}$ (b), and and the scaled electric force F^*_E (c) as a function of the scaled pore radius S/a_0 at various values of $^d/_a$ for the case in which $\zeta_p = 0$, $\zeta_w = 1$, and $\kappa a_0 = 1$.

only the z components of these forces, F_D and F_E, respectively, need be considered. These forces can be calculated by[20,21]

$$F_E = \int\int_{\Omega} \sigma_p E_z \, ds = \int\int_{\Omega} \sigma_p \left(\frac{\partial \Psi}{\partial z}\right) d\Omega \qquad (16)$$

$$F_D = \int\int_{\Omega} \eta \frac{\partial(\mathbf{u}\cdot\mathbf{t})}{\partial n} t_z \, d\Omega + \int\int_{P} -p n_z \, d\Omega \qquad (17)$$

where Ω denotes the ellipsoid surface and t_z and n_z are the z components of $\mathbf{t}$ and $\mathbf{n}$, respectively, with $\mathbf{t}$ being the unit tangential vector on the ellipsoid surface. At steady state, $F_E + F_D = 0$. U is calculated by the method proposed by O'Brien and White[22] where the present problem is decomposed into two subproblems. In the first subproblem, an ellipsoid moves with a constant velocity U in the absence of $\mathbf{E}$; therefore, it experiences a conventional hydrodynamic drag $F_{D,1} = -UD$, where D is the drag per unit velocity that depends only on the geometry of the problem. In

(20) Hsu, J. P.; Yeh, L. H. *J. Chin. Inst. Chem. Eng.* **2006**, *37*, 601.
(21) Hsu, J. P.; Yeh, L. H.; Ku, M. H. *J. Colloid Interface Sci.* **2007**, *305*, 324.
(22) O'Brien, R. W.; White, L. R. *J. Chem. Soc., Faraday Trans. 2* **1978**, *74*, 1607.

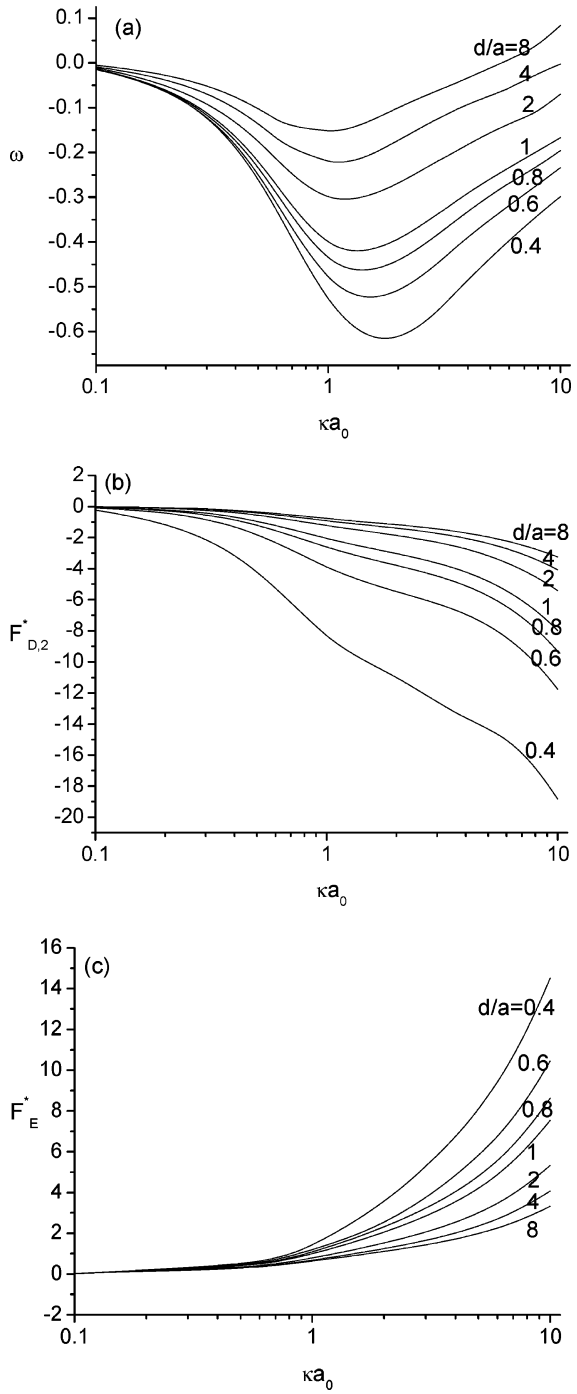

Figure 9. Variation of the scaled mobility of an ellipsoid ω (a), the scaled hydrodynamic force $F^*_{D,2}$ (b), and the scaled electric force F^*_E (c), as a function of the scaled double layer thickness κa_0 at various values of $^d/_a$ for the case in which $\zeta_p = 1$, $\zeta_w = 1$, and $S = 3a_0$.

the second subproblem, **E** is applied, but an ellipsoid is held fixed in the space. In this case, the ellipsoid experiences two forces: the electric force F_E and an extra hydrodynamic force arising from the moving of the ionic species in the double layer $F_{D,2}$, which can be either a driving force or a retardation force, depending on the boundary conditions of the electric field. Because $F_D = F_{D,1} + F_{D,2}$, $F_E + F_D = 0$ leads to

$$U = \frac{F_E + F_{D,2}}{D} \tag{18}$$

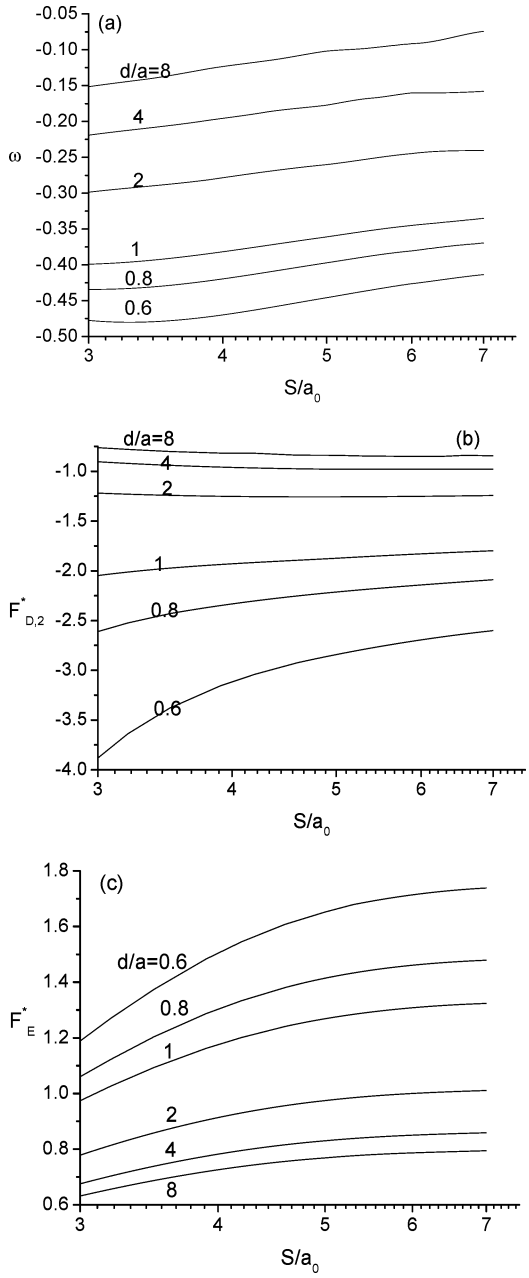

Figure 10. Variation of the scaled mobility of an ellipsoid ω (a), the scaled hydrodynamic force $F^*_{D,2}$ (b), and the scaled electric force F^*_E (c), as a function of the scaled pore radius S/a_0 at various values of $^d/_a$ for the case in which $\zeta_p = 1$, $\zeta_w = 1$, and $\kappa a_0 = 1$.

U is evaluated by the following procedure: (i) Substituting $\Psi = \Psi_1 + \Psi_2 = 0$ into eq 6, solving the resultant expression simultaneously with eq 7, and substituting the result obtained into eq 17 to evaluate $F_{D,1}$. (ii) Solving eqs 4 and 5 subject to eqs 8−10 or 10−12 to obtain Ψ_1 and Ψ_2, and substituing the results into eq 16 to calculated F_E. (iii) Substituting Ψ_1 and Ψ_2 obtained in the previous step into eq 6, solving the resultant expression simultaneously with eq 7, and then using eq 17 to evaluate $F_{D,2}$. (iv) Substituting F_E, $F_{D,1}$, and $F_{D,2}$ thus obtained into eq 18 to obtain U.

Results and Discussion

For a simpler representation, we define the following: $\omega = U/\epsilon(k_BT/e)^2/a_0$, the scaled mobility of an ellipsoid; $D^* = D/6\pi\epsilon$-$(k_BT/e)^2$, the scaled conventional hydrodynamic drag per unit

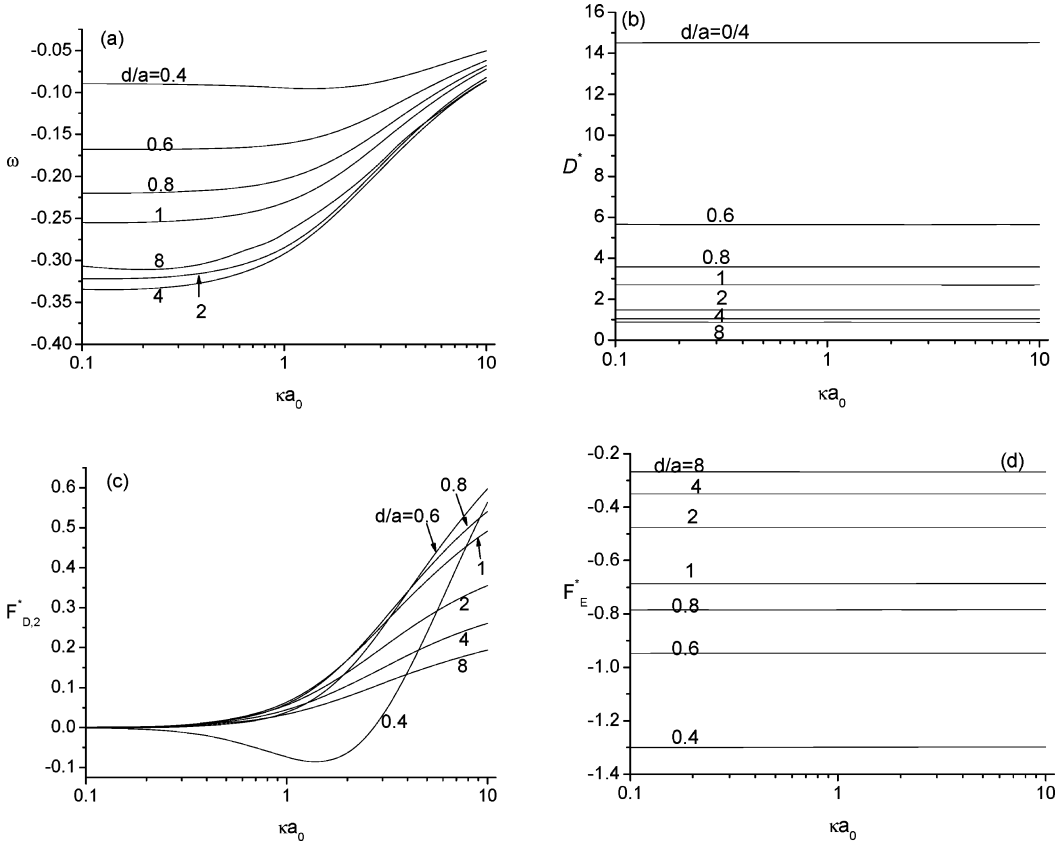

Figure 11. Variation of the scaled mobility of an ellipsoid ω (a), the scaled drag coefficient D^* (b), the scaled hydrodynamic force $F^*_{D,2}$ (c), and the scaled electric force F^*_E (d) as a function of the scaled pore radius κa_0 at various values of $^d/_a$ for the case in which $\sigma_p = -1$, $\zeta_w = 0$, and $S = 3a_0$.

velocity of an ellipsoid; $F^*_{D,2} = F_{D,2}/6\pi\epsilon(k_BT/e)^2$, the scaled hydrodynamic force acting on an ellipsoid arising from the movement of the ionic species in a double layer; and $F^*_E = F_E/6\pi\epsilon(k_BT/e)^2$, the scaled electric force acting on an ellipsoid. Note that $\omega = (F^*_E + F^*_{D,2})/D^*$.

FlexPDE,[23] a differential equation solver based on a finite element method, is adopted to solving the governing equations and the associated boundary conditions. Double precision is used throughout the computation, and grid independence is checked to ensure that the mesh used is fine enough. Typically, 6000 and 3500 nodes are necessary for the resolution of the electric field and the flow field, respectively. Figure 2 shows the typical mesh structure where an unstructured triangular mesh is used with a finer mesh near the ellipsoid and a coarser mesh away from it. The applicability of the software adopted is justified by considering the electrophoresis of a sphere of radius R along the axis of a cylindrical pore. Figure 3 shows the simulated variation of ω as a function of $^S/_R$ on the basis of the present method and the corresponding results of Ennis and Anderson[24] and Shugai and Carnie;[25] the former is accurate when $^S/_R$ is small, and the latter is accurate when $^S/_R$ is large. Figure 3 reveals that the software adopted in this study is appropriate for the description of the behavior of ω for the entire range of $^S/_R$.

For convenience, we assume the volume of an ellipsoid is fixed at $4\pi a_0^3/3$ in the subsequent discussion.

$\zeta_p = 1$ and $\zeta_w = 0$. Let us consider first the case of an ellipsoid with constant, positive surface potential in an uncharged pore. Figure 4a reveals that for a fixed aspect ratio $^d/_a$, the scaled electrophoretic mobility ω increases with the increasing κa_0. This is because if a_0 is fixed then a larger κa_0 implies a higher electrolyte concentration and a thinner double layer. According to Figure 4b, because D^* is insensitive to the variation in κa_0, it is not the major factor affecting the qualitative behavior of ω. However, both $|F^*_{D,2}|$ and F^*_E vary appreciably with κa_0, and the latter dominates. Therefore, the qualitative behavior of ω depends mainly on that of F^*_E. Figure 4a also reveals that for a fixed κa_0, ω (oblate) > ω (sphere) > ω (prolate). This is because $\omega = (F^*_E + F^*_{D,2})/D^*$, and among F^*_E, $F^*_{D,2}$, and D^*, D^* is the dominating factor, as seen in Figure 4b−d. For the present case, both D^* and F^*_E are positive with D^*(prolate) > D^*(sphere) > D^*(oblate) and F^*_E (prolate) > F^*_E (sphere) > F^*_E (oblate). However, no general trend can be found for $F^*_{D,2}$. Note that if $^d/_a = 0.4$ then $F^*_{D,2}$ has a local maximum as κa_0 varies. Also, $F^*_{D,2}$ is positive if κa_0 is small and is negative if κa_0 is large. This is because if the double layer is thick then the pressure on an ellipsoid is more important than the viscous force, but the reverse is true if the double layer is thin. For values of $^d/_a$ other than 0.4, $F^*_{D,2}$ is negative. The trend in D^* arises from the fact that when the volume of an ellipsoid is fixed its projection area on the plane perpendicular to the z axis as $^d/_a$ varies in rank as follows: prolate > sphere > oblate, as shown in Figure 5. The trend in F^*_E can be explained by the fact that if the volume of an ellipsoid is fixed then its surface areas $^d/_a$ varies in rank as follows: prolate > sphere > oblate, as illustrated in Figure 5. The larger the surface area, the higher the charge on the surface and therefore the greater the F^*_E.

As seen in Figure 6, ω increases with increasing S/a_0, which is expected because the larger the S/a_0, the smaller the

(23) *FlexPDE*, version 2.22; PDE Solutions Inc.: Spokane Valley, WA, 2003.
(24) Ennis, J.; Anderson, J. L. *J. Colloid Interface Sci.* **1997**, *185*, 497.
(25) Shugai, A. A.; Carnie, S. L. *J. Colloid Interface Sci.* **1999**, *213*, 298.

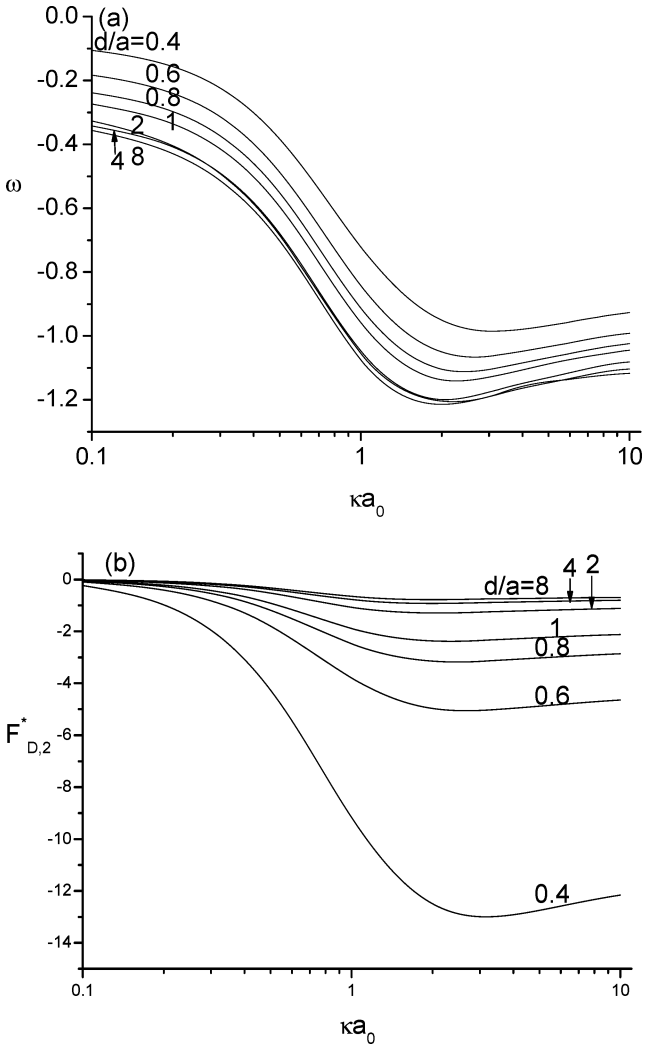

Figure 12. Variation of the scaled mobility of an ellipsoid ω (a) and the scaled hydrodynamic force $F^*_{D,2}$ (b) as a function of the scaled double-layer thickness κa_0 at various values of $^d/_a$ for the case in which $\sigma_p = -1$, $\zeta_w = 1$, and $S = 3a_0$.

hydrodynamic retardation due to the presence of the cylindrical pore. For a fixed scaled radius of a pore S/a_0, ω (oblate) > ω (sphere) > ω (prolate). This is because the magnitude of $F^*_{D,2}$ is relatively unimportant when compared to that of D^* or F^*_E. Also, D^*(prolate) > D^*(sphere) > D^*(oblate) and F^*_E (oblate) > F^*_E (sphere) > F^*_E (prolate). $F^*_{D,2}$ is negative except for the case where $^d/_a = 0.4$, where it is positive if S/a_0 is small and becomes negative if S/a_0 is large. This is because if the radius of a pore is small then the pressure on an ellipsoid is more important than the corresponding viscous force, but the reverse is true if the radius of the pore is large. Figure 6e illustrates the variation of the ratio $R = \omega$ (present study)/ω (Yoon and Kim)[9] as a function of S/a_0 for various combinations of $^d/_a$ and κa_0. Because the results of Yoon and Kim[9] are based on an isolated particle, R is a measure of the significance of the boundary effect; the closer its value is to unity, the less significant the presence of the pore. As expected, the smaller the $^d/_a$ and/or the smaller the κa_0, the more important the boundary effect. For the present case, this effect should not be neglected if S/a_0 is smaller than about 15.

$\zeta_p = 0$ and $\zeta_w = 1$. Consider next the case where an uncharged ellipsoid is in a cylindrical pore of constant, positive surface potential. Note that because D^* is independent of the charged conditions on the surfaces, the D^* in the present case is the same as that shown in Figure 4b. In the present case, because a negative charge is induced on the ellipsoid surface as it approaches the pore surface, ω is negative and $F^*_{D,2}$ becomes a scaled driving force. Note that $|\omega|$ has a local maximum near $\kappa a_0 \cong 2$, as shown in Figure 7a. The presence of the local maximum is the net result of the competition of the scaled forces D^*, F^*_E, and $F^*_{D,2}$, illustrated in Figures 4b and 7c,b, respectively. For the present case, $|\omega|$ (oblate) > $|\omega|$ (sphere) > $|\omega|$ (prolate), which arises mainly from D^*(prolate) > D^*(sphere) > D^*(oblate).

The influence of the pore on the behavior of the ellipsoid is summarized in Figure 8. In this case, D^* is the same as that shown in Figure 6b. Similar to the case of Figure 6a, the larger the S/a_0, the larger the $|\omega|$. This is because although the scaled driving forces $|F^*_E|$ and $|F^*_{D,2}|$ decline with the increasing S/a_0, the scaled drag D^* decreases at the same time. The decline in $|F^*_{D,2}|$ as S/a_0 increases, as observed in Figure 8b, arises from the negative charge induced on the surface of the ellipsoid, and the larger the S/a_0, the smaller the amount of induced charge. As in the case of Figure 4a, the aspect ratio $^d/_a$ varies, and we have $|\omega|$ (oblate) > $|\omega|$ (sphere) > $|\omega|$ (prolate), which arises mainly from D^*(prolate) > D^*(sphere) > D^*(oblate).

$\zeta_p = 1$ and $\zeta_w = 1$. In this case, both the ellipsoid and the cylindrical pore have a constant positive surface potential. Note that D^* is the same as that shown in Figure 4b. Figure 9a reveals that ω has a negative local minimum near $\kappa a_0 \cong 1.5$. The presence of this local minimum is the net result of the competition of the scaled forces D^*, $F^*_{D,2}$, and F^*_E. Figure 9a suggests that if $^d/_a$ is sufficiently large ($^d/_a > 4$) ω may change its sign from negative to positive as κa_0 increases, which can be justified by comparing the magnitudes of D^*, $F^*_{D,2}$, and F^*_E. If ω is negative, where κa_0 takes a small to medium value, then $|\omega|$ (oblate) > $|\omega|$ (sphere) > $|\omega|$ (prolate), but if ω is positive, where κa_0 is large, then $|\omega|$ (prolate) > $|\omega|$ (sphere) > $|\omega|$ (oblate). These can be explained by the variations of D^*, $F^*_{D,2}$, and F^*_E shown in Figures 4b and 9b,c, respectively.

The influence of the cylindrical pore on the behavior of the ellipsoid is summarized in Figure 10. In this case, D^* is the same as that shown in Figure 6b. Figure 10a shows that $|\omega|$ decreases with increasing S/a_0, which arises from the fact that as S/a_0 increases the rate of decrease of the net driving force ($F^*_{D,2} + F^*_E$) is faster than that of the drag force. A comparison between parts b and c of Figure 10 reveals that $F^*_E < |F^*_{D,2}|$ for the present case. Note that, because of the linear nature of the present problem, $F^*_{D,2}$ in Figure 10b can be obtained by summing the terms in Figures 6c and 8b. $|F^*_{D,2}|$ is seen to decline with increasing S/a_0, as does $|\omega|$. The former can be explained by the same reasoning as that employed in the discussion of Figure 8b. Figure 10a indicates that $|\omega|$ (prolate) > $|\omega|$ (sphere) > $|\omega|$ (oblate). As can be concluded from Figures 6b and 10b,c, this is because the total driving force ($F^*_E + F^*_{D,2}$) dominates.

$\sigma_p = -1$ and $\zeta_w = 0$. Here, the ellipsoid has a constant negative surface charge density, and the cylindrical pore is uncharged. For the present case, D^* is the same as that shown in Figure 4b. According to Figures 4b and 11d, because both D^* and F^*_E are insensitive to the variation of κa_0, the qualitative behavior of ω depends mainly on that of $F^*_{D,2}$, which decreases with the increase in κa_0, in general. Because the electric force acting on the ellipsoid is fixed in the present case, $|\omega|$ declines with the increasing κa_0. Figure 11a indicates that for a fixed κa_0, $|\omega|$ (oblate) > $|\omega|$ (sphere) > $|\omega|$ (prolate). This is because D^* dominates in the present case, and, as shown in Figure 4b, D^*-(prolate) > D^*(sphere) > D^*(oblate). Note that because the ellipsoid is negatively charged $F^*_{D,2}$ is positive, in general, except when $^d/_a = 0.4$, where $F^*_{D,2}$ has a negative local minimum

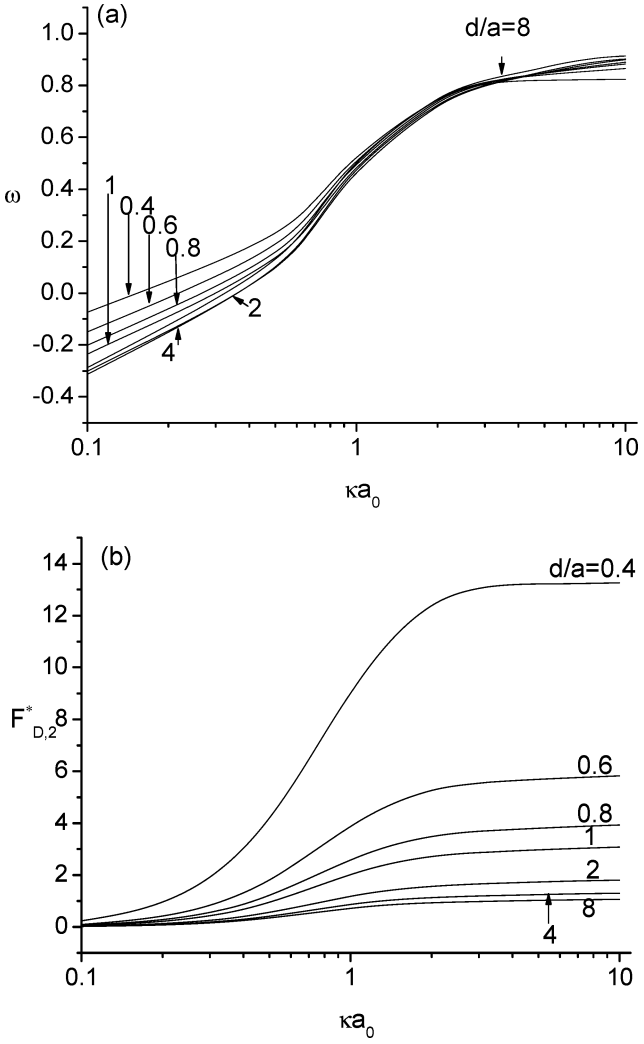

Figure 13. Variation of the scaled mobility of an ellipsoid ω (a) and the scaled hydrodynamic force $F^*_{D,2}$ (b) as a function of the scaled double-layer thickness κa_0 at various values of $^d/_a$ for the case in which $\sigma_p = -1$, $\zeta_w = -1$, and $S = 3a_0$.

as κa_0 varies. As mentioned previously, this arises from the fact that if the double layer is thick then the pressure is more important than the viscous force, but the reverse is true if it is thin. Note that both the pressure and the viscous force decrease with increasing κa_0 and the rate decrease of the former is faster than that of the latter.

$\sigma_p = -1$ and $\zeta_w = 1$. In this case, the ellipsoid has a constant negative surface charge density, and the cylindrical pore has a constant positive surface potential. Here, D^* is the same as that shown in Figure 4b. Also, according to eq 16 F^*_E is independent of the charge conditions on the pore surface; therefore, F^*_E is the same as that shown in Figure 11d. Note that $F^*_{D,2}$ is negative and is a scaled driving force. Figure 12a reveals that ω has a local minimum at $\kappa a_0 \cong 2$. This is because F^*_E is insensitive to the variation in κa_0 and the qualitative behavior of ω is mainly dominated by $F^*_{D,2}$. If $\kappa a_0 < 2$, then $|F^*_{D,2}|$ increases with increasing κa_0, but this trend is reversed if $\kappa a_0 > 2$. Figure 12a also indicates that $|\omega|$ (oblate) > $|\omega|$ (sphere) > $|\omega|$ (prolate). Again, this is because D^* dominates the magnitude of ω, and D^*(prolate) > D^*(sphere) > D^*(oblate).

$\sigma_p = -1$ and $\zeta_w = -1$. Let us consider next the case where the ellipsoid has a constant negative surface charge density and the pore has a constant negative surface potential. Here, D^* and F^*_E are the same as shown in Figures 4b and 11d, respectively. If κa_0 is small, then ω is negative, but it becomes positive if κa_0 is sufficiently large. As illustrated in Figures 11d and 13b, this is because if κa_0 is small, then negative F^*_E dominates, and if κa_0 is sufficiently large, then positive $F^*_{D,2}$ dominates. Note that the ω curves of the ellipsoids of various aspect ratios cross each other at $\kappa a_0 \cong 3$.

Conclusions

The influence of a charged boundary on the electrophoretic behavior of a particle is analyzed by considering the electrophoresis of an ellipsoid along the axis of a cylindrical pore. We show that the behavior of a particle is much more complicated and interesting compared with that for the case where the boundary is uncharged. The results of numerical simulation can be summarized as follows. (i) If an ellipsoid of constant positive surface potential is placed in an uncharged cylindrical pore, then the scaled electrophoretic mobility increases with the decreasing thickness of the double layer. The mobilities of various types of ellipsoid rank as follows: oblate > sphere > prolate. The presence of the pore has the effect of decreasing the mobility. (ii) For the case of an uncharged ellipsoid and a cylindrical pore of constant positive surface potential, the absolute value of the mobility has a local maximum at a moderately thick double layer. For the present case, the absolute values of the mobilities of various types of ellipsoids rank as follows: oblate > sphere > prolate. (iii) If both the ellipsoid and the cylindrical pore have a constant positive surface potential, then the mobility shows a negative local minimum at a moderately thick double layer. For oblates, if the aspect ratio is sufficiently large, then the mobility may change its sign from negative to positive as the thickness of the double layer increases. If the mobility is negative, then the absolute values of the mobilities of various types of ellipsoid rank as follows: oblate > sphere > prolate. If the mobility is positive, then that order is reversed. In the present case, the presence of the pore has the effect of increasing the absolute value of the mobility. (iv) For the case where an ellipsoid of constant negative surface charge density is in an uncharged pore, regardless of the aspect ratio, the absolute value of the mobility always declines with the decrease in the thickness of the double layer. For a fixed double-layer thickness, the absolute values of the mobility of various types of particles rank as follows: oblate > sphere > prolate. (v) For the case where the ellipsoid has a constant negative surface charge density and the cylindrical pore has a constant positive surface potential, the mobility has a local minimum at a moderately thick double layer. In this case, the absolute values of the mobility of various types of particles rank as follows: oblate > sphere > prolate. (vi) If the ellipsoid remains at a constant negative surface charge density and the pore remains at a constant negative surface potential, then the mobility is negative when the double layer is thick, but it becomes positive if it is sufficiently thin.

Acknowledgment. This work is supported by the National Science Council of the Republic of China.

LA703195F